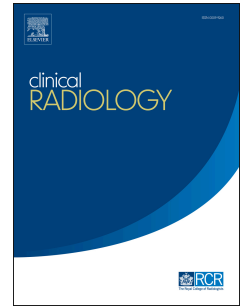


Journal Pre-proof

The utility of Dynamic Contrast Enhanced Intranodal MR Lymphangiography in the investigation of primary lymphatic anomalies.

Ratnam L.A., Mills M., Wale A., Howroyd L.R., Itkin M., Howe F.A., Gordon K., Mansour S., Ostergaard P., Mortimer P.S.



PII: S0009-9260(24)00298-8

DOI: <https://doi.org/10.1016/j.crad.2024.06.009>

Reference: YCRAD 6629

To appear in: *Clinical Radiology*

Received Date: 24 January 2024

Revised Date: 18 May 2024

Accepted Date: 1 June 2024

Please cite this article as: Ratnam L, Mills M, Wale A, Howroyd L, Itkin M, Howe F, Gordon K, Mansour S, Ostergaard P, Mortimer P, The utility of Dynamic Contrast Enhanced Intranodal MR Lymphangiography in the investigation of primary lymphatic anomalies., *Clinical Radiology*, <https://doi.org/10.1016/j.crad.2024.06.009>.

This is a PDF file of an article that has undergone enhancements after acceptance, such as the addition of a cover page and metadata, and formatting for readability, but it is not yet the definitive version of record. This version will undergo additional copyediting, typesetting and review before it is published in its final form, but we are providing this version to give early visibility of the article. Please note that, during the production process, errors may be discovered which could affect the content, and all legal disclaimers that apply to the journal pertain.

© 2024 Published by Elsevier Ltd on behalf of The Royal College of Radiologists.

Author Contributions:

1 guarantor of integrity of the entire study. Ratnam

2 study concepts and design. Ratnam, Mills, Wale, Itkin, Howe.

3 literature research. Ratnam, Wale, Mills, Howroyd

4 clinical studies. Ratnam, Howroyd, Mills

5 experimental studies / data analysis. Ratnam, Mills, Wale, Howroyd

6 statistical analysis. Ratnam

7 manuscript preparation. Ratnam, Mills, Wale, Howroyd

8 manuscript editing. Ratnam, Mills, Wale, Howroyd, Howe, Gordon, Mansour, Ostergaard,

Mortimer

TITLE PAGE

Manuscript Title

The utility of Dynamic Contrast Enhanced Intranodal MR Lymphangiography in the investigation of primary lymphatic anomalies.

Manuscript Type: Technical report

Authors

Ratnam LA^{1,2}, Mills M², Wale A^{1,2}, Howroyd LR^{1,2}, Itkin, M⁵, Howe FA², Gordon K^{2,3}, Mansour S^{2,4}, Ostergaard P², Mortimer PS^{2,3}

1 Department of Radiology, St George's University Hospitals NHS Foundation Trust, London SW17 0QT, UK

2 Molecular and Clinical Sciences Research Institute, St George's University of London, London SW17 0RE, UK

3 Dermatology and Lymphovascular Medicine, St George's University Hospitals NHS Foundation Trust, London SW17 0QT, UK

4 South West Thames Centre for Genomics, St George's University Hospitals NHS Foundation Trust, London, UK

5 Department of Radiology, University of Pennsylvania Health System, Philadelphia, USA.

Corresponding authors

Dr LA Ratnam, lakshmi.ratnam@stgeorges.nhs.uk, for technical correspondence and Prof S Mansour, smansour@sgul.ac.uk, for clinical queries.

Acknowledgements

We would like to thank Professor Robert Morgan for his advice and assistance in the submission of this manuscript. We would also like to thank Professor Vaughan Keeley and Dr Katie Riches from Derby Hospitals NHS Foundation Trust for their support with the patient identification stage of the project.

Funding information:

1. This paper has been supported by a joint grant from the Medical Research Council (MRC) and the British Heart Foundation (BHF) (MR/P011543/1 and RG/17/7/33217), with no direct involvement of these sponsors.
2. The authors declare that they have no conflict of interest.

Abbreviations:

CNR – Contrast-to-noise ratio

DCMRL – Dynamic Contrast Enhanced Intranodal Magnetic Resonance Lymphangiography

MIP – Maximum Intensity Projection

MR – Magnetic resonance

MRA – Magnetic Resonance Angiography

MRL – Magnetic Resonance Lymphangiography

SCID – Severe combined immunodeficiency

SPGR – Spoiled Gradient Echo

TD – Thoracic Duct

The utility of Dynamic Contrast Enhanced Intranodal MR Lymphangiography in the investigation of primary lymphatic anomalies.

Abstract

Background: Primary lymphatic anomalies are often complicated by central lymphatic abnormalities. Intranodal dynamic contrast enhanced MR lymphangiography (DCMRL) is a relatively new technique for imaging the central lymphatic system. Historically, the only method of imaging the central lymphatics well was with pedal lymphangiography, which is technically challenging, time consuming, involves the use of ionising radiation and has risks associated with the use of lipiodol. The treatment options for primary lymphatic disorders have also been limited to symptomatic management.

Purpose: To describe the technique of DCMRL to identify central lymphatic abnormalities in patients with primary lymphatic anomalies and discuss utility of the findings.

Materials and Methods: 28 patients with primary lymphatic abnormalities underwent dynamic MR imaging following injection of gadolinium directly into inguinal lymph nodes at a tertiary lymphovascular referral centre.

Results: Technical success was achieved in 23 patients (82.1%). Pathological imaging findings included obstructed, hypoplastic or absent lymphatic channels with collateralisation/rerouting or reflux of flow, lymphangiectasia, lymphatic pseudoaneurysms and lymph leaks. Protocol modifications for improved imaging are highlighted including technical aspects of lymph node injection, image acquisition and MRI parameters. In two patients, imaging findings warranted embolization of the abnormal lymphatic channels with subsequent symptomatic improvement.

Conclusion: DCMRL has been shown to be a safe, reproducible technique in patients with primary lymphatic anomalies enabling imaging of the central lymphatic system.

1 **The utility of Dynamic Contrast Enhanced Intranodal MR Lymphangiography in the**
2 **investigation of primary lymphatic anomalies.**

3 **Introduction**

4 Intranodal dynamic contrast enhanced MR lymphangiography (DCMRL) is a relatively new technique
5 enabling imaging of the central lymphatics via injection of contrast directly into inguinal lymph
6 nodes. Lymphoscintigraphy remains the investigation of choice for diagnosis in lymphatic disorders
7 but does not give detailed imaging of the central lymphatics.^{1–3} Pedal lymphangiography with
8 Lipiodol whereby contrast was injected directly into lymphatics in the foot which had been surgically
9 exposed is invasive, very time consuming, involves ionising radiation, and can result in lipiodol
10 embolization.⁴ XXXXXXX NHS Foundation Trust is recognised as a national referral centre in the UK
11 for Primary Lymphatic Anomalies. Many of these genetically determined forms of primary lymphatic
12 anomalies have central lymphatic abnormalities associated with (or causing) peripheral
13 lymphoedema.^{5–8} These lymphatic abnormalities may not be clinically obvious yet are important to
14 diagnose both for correct phenotyping and for ongoing management.⁹ Although described for other
15 indications, there remains a paucity of data exploring DCMRL's utility in patients with primary
16 lymphatic anomalies.^{10–12} The purpose of this paper is to describe the method and utility of this
17 technique in imaging central lymphatic abnormalities in patients with primary lymphatic anomalies.

18 **Materials and Methods**

19 **Patients**

20 Patients were referred for DCMRL if they had a diagnosis of a primary lymphatic anomaly (chylous
21 reflux, significant lymphoedema with a suggestion of obstruction on lymphoscintigraphy,
22 chylothorax, chylopericardium or chylous ascites).

23 **DCMRL technique**

24 Inguinal lymph node puncture was carried out under ultrasound guidance using a shallow angle of
25 entry with a long subcutaneous tract to obtain a stable needle position with a 23G spinal needle (BD,
26 Franklin Lakes, NJ). Ideally, a minimum of one needle was sited in each groin. Where nodes were

27 easily visualised and patients tolerated placement well, a third needle was sited to increase likelihood
28 of contrast uptake. Satisfactory position within the lymph node was then confirmed using injection of
29 1ml of SonoVue (sulphur hexafluoride microbubbles) ultrasound contrast (Bracco Spa, Milan, Italy)
30 mixed with 2ml of 0.25% Chirocaine (levobupivacaine) for local anaesthesia. The needles were then
31 secured in place with dressings and connecting tubing attached with syringes primed with Gadoteric
32 acid (Dotarem®; Guerbet, France).

33 Magnetic Resonance Imaging

34 For all studies, MR imaging was performed using a clinical 3.0T MRI system Philips Achieva 3.0T TX
35 and a 16-element phased array torso coil for signal reception. The imaging protocol (**Table 1**) consists
36 of initial non-contrast sequences followed by dynamic contrast enhanced imaging.

37 Non-contrast imaging of the abdomen and pelvis begins with a 2D T₂-weighted breath-held turbo spin
38 echo (TSE) acquisition for identification of gross abnormalities (e.g., fluid accumulations), 3D image
39 planning, and allows for the identification of incidental findings. A 3D heavily T₂-weighted TSE
40 sequence follows, for which only very long T₂ compartments retain reasonable signal intensity. Finally,
41 a pre-contrast 3D T₁-weighted spoiled gradient echo (SPGR) image was acquired. The non-contrast T₂-
42 weighted images were assessed for the presence or absence of ascites, pleural and pericardial effusions,
43 oedema in the soft tissues and the presence of masses of lymphatic nature, and for how well the
44 lymphatics were visualised.

45 Slow injection (over 1-2 minutes) of 4 - 9ml of undiluted 279.32 mg/ml Gadoteric acid (Dotarem®;
46 Guerbet, France) was then carried out simultaneously via each needle placed in an inguinal lymph node,
47 followed by dynamic T₁-weighted imaging post-injection to depict contrast dispersion over time (each
48 acquisition lasted 0.5 minutes). A maximum of 3 needles were placed and maximum total dose of 18ml
49 of Gadoteric acid injected. In cases where contrast was initially difficult to visualise, T₁-weighted
50 Dixon images, of higher spatial resolution and larger field of view than the spoiled gradient echo
51 sequences, were acquired. Imaging initially focussed on the pelvis and lower abdomen until contrast
52 was seen to leave this region (variable), at which point the coil was repositioned to continue imaging to

53 the thoracic duct termination. The post-contrast T1weighted images were evaluated for presence or
54 absence of lymphatic vessels, anatomical distribution of the contrast (normal or abnormal), reflux,
55 lymphatic pseudoaneurysms, leakage of lymphatic fluid, rerouting/ collateralisation, and the presence
56 of dermal backflow of contrast. All image volumes were reformatted as maximum intensity projections
57 (MIPs) for review, coronal projections for T₁-weighted image series and radial projections for the T₂-
58 weighted images. Total imaging time ranged from approx. 30 – 90 minutes, however an hour was typical
59 (average \pm standard deviation = 53 \pm 13 min), variability was secondary to individual variation in the
60 post-contrast acquisition time.

61

62 **Results**

63 From January 2018 to December 2022, 28 patients were imaged. A summary of the results and
64 underlying primary lymphatic diagnosis is provided in **Table 2**. The imaging findings are described
65 below. No contrast reactions were observed and no patients terminated the examination due to pain,
66 no delayed complications were reported during post procedure follow-up.

67

68 Non contrast:

69 From the T2 non-contrast imaging, central lymphatic channels could not be identified in 10 of the 28
70 patients. Of the remaining 18 patients, the lymphatic channels could be seen but were faint and not
71 deemed to be sufficiently visualised to be diagnostically helpful in 16 patients [**Figure 1**]. The
72 lymphatic channels were seen well in only two patients [**Figure 2a**].

73

74 Post contrast:

75 Technical success visualising the central lymphatics was achieved in 23 patients (82.1%). In five
76 patients, injection was performed unilaterally due to absence/ inability to identify targetable lymph

77 nodes on the contralateral groin either due to previous surgical removal of nodes or extensive oedema
78 [Table 2]. Central lymphatics were successfully visualised in all five patients with contrast noted on
79 the non-injected side signifying reflux (Cases 10, 26 and 28) [Figure 2b], normal unilateral uptake
80 with normal thoracic duct (Case 20), and superficial re-routing indicating obstructed main drainage
81 routes (Case 13).

82 In the remaining 23 patients, bilateral injections were performed. Of these,

- 83 a) In 5 patients (Cases 1, 2, 9, 15 and 17), no propagation of contrast was seen bilaterally. These
84 were considered technical failures.
- 85 b) In 3 patients (Cases 5, 16, and 19), bilateral uptake of contrast was noted, and the imaging
86 showed normal central lymphatics.
- 87 c) In 6 patients (Cases 3, 6, 7, 8, 11, and 25), bilateral uptake of contrast was noted with
88 abnormalities detected (termination of the thoracic duct (TD), absent filling of TD,
89 lymphopseudoaneurysms, lymphangiectasia, obstructed or absent lymphatic channels with
90 collateralisation).
- 91 d) In 9 patients, propagation of contrast was absent on **one** of the injected sides in the groin
92 (bilateral injections performed). Of these, 2 patients (Cases 21 and 22) showed normal lumbar
93 and iliac lymphatics on the side with contrast propagation with normal appearances of the TD.
94 The remaining 7 had a range of abnormalities including reflux into the ipsilateral pelvis and
95 limb which was the limb affected with lymphoedema (Case 23), collateralisation with re-
96 routing of the lymphatic fluid to the distal lymphatic channels (Cases 14, 18 and 27) and
97 lymphopseudoaneurysms (Cases 12 and 24) and a patient with Noonan syndrome with
98 abnormal mediastinal and pulmonary lymphatic perfusion and rapid flow of contrast to the
99 terminal TD (Case 4).

100 Discussion

101 The ability to image the central lymphatic system in this group of patients has led to an understanding
102 of the anatomy of their central lymphatics which was previously unknown. The discussion is divided
103 into technical factors and the lymphatic findings.

104 1. Review of DCMRL procedures

105 **Selection of lymph node for contrast injection:** Subjectively abnormal, absent and hypoplastic
106 lymph nodes are more common in patients with primary lymphatic disorders with target nodes
107 frequently < 1cm in size. Ideal needle tip positioning is at the corticomedullary junction. Lymph node
108 enhancement and efferent flow after injection of ultrasound contrast confirms good positioning. 13–15
109 The chirocaine alleviates pain that is otherwise experienced on injection of Gadoteric acid
110 intranodally.

111 **Securing the needles in position:** We noted ease of needle displacement in our initial studies (loss of
112 position between placement and fixation, extravasation noted in the groin) with no uptake of contrast
113 on the displaced side. Thus, if patients tolerated needle placement well, up to 3 needles in one groin
114 were placed to maximise chances of introducing contrast into lymph nodes. This was only carried out
115 in 3 patients. Initial studies had an attempted injection of 9 ml of Gadoteric acid into each node,
116 however reduction to 4 ml injected into each node was found to still provide satisfactory contrast
117 visualisation with improved tolerance from patients. We found that avoiding placement of needles in
118 the groin crease, positioning the coil above the tip of the needles and the use of connecting tubing
119 primed with contrast and attached at needle placement also stops the needles becoming displaced
120 when connecting a syringe to the needle for injection in the MRI scanner.

121 **Non-contrast T₂ weighted Magnetic Resonance Imaging:** Unlike most bodily tissues, lymph can be
122 expected to retain reasonable signal in long echo time scans given its T₂ time of approx. 610 msec at
123 3T16. These images provide a high contrast-to-noise ratio (CNR) for fluid containing regions and are
124 thus especially useful for identifying areas of lymphatic fluid accumulation [Figure 3]. Despite a
125 reduced CNR, moderately T₂-weighted 2D sequences were also found to be beneficial as the fluid

126 accumulations could be observed in the context of the underlying anatomy. Sites setting up their own
127 MRL protocols may wish to consider whether two acquisitions are required in their context,
128 particularly if scanner time is limited. Acceleration techniques such as partial Fourier reconstruction
129 can also be applied to reduce imaging time but can reduce image SNR and introduce artefacts.¹⁷
130 Other non-contrast approaches have been described to assess the lymphatics in the abdomen
131 including a recent attempt using balanced steady state free-process (bSSFP).¹⁸ In this paper, cardiac
132 triggered and respiratory navigated bSSFP images facilitated improved visualisation of the
133 lymphatics compared to respiratory triggered heavily T₂ weighted TSE. bSSFP sequences exhibit a
134 complex T₂/T₁ weighting in which fluids (lymph, CSF, blood) are high signal. We therefore chose not
135 to employ bSSFP over TSE given the high blood signal which could cause confusion in differentiating
136 lymphatic from the vascular structures.

137 **Contrast-enhanced T₁-weighted Magnetic Resonance Imaging:** Administration of Gadoteric acid
138 into the lymphatics reduces the long T₁ time of lymph sufficiently to be observed in dynamic T₁-
139 weighted images where the passage of contrast agent within the lymphatics needs to be observed over
140 time [Figure 3].¹⁶ We employed Gadoteric acid due to a combination of local availability and its
141 strong safety profile.¹⁹ Similar enhancement with a reduced volume of contrast agent may be possible
142 using a similarly safe agent with greater r₁ relaxivity such as Gadoteridol or Gadobutrol²⁰ but
143 requires *in-vivo* validation for lymphatic applications.

144 With high spatial and temporal resolution [Table 1], the spoiled gradient echo sequence was the
145 default sequence for our dynamic imaging, Dixon based images are less affected by inhomogeneities
146 outside the scanner isocentre but maintain high quality fat suppression, DIXON imaging was acquired
147 in several cases and were particularly useful for cases in which contrast agent was seen to re-route via
148 superficial lymphatic vessels [Figure 4]. A spoiled gradient echo sequence was chosen as the
149 standard sequence for the dynamic post-contrast imaging as DIXON imaging takes longer to
150 reconstruct and therefore limits the ability for on-table evaluation of the findings.

151 Some sites performing DCMRL have employed keyhole imaging to accelerate their T₁-weighted
152 dynamic imaging²¹. However, care must be taken to ensure sufficient high spatial frequency data is
153 captured to appropriately reconstruct small structures such as lymphatics and further work in this area
154 is required. Additionally, methods of motion artefact reduction have been employed by several centres
155 (breath-held T₁-weighted contrast enhanced scans, and respiratory or cardiac gating/triggering T₂
156 scans) to reduce motion artefacts and improve image quality, at the expense of extend imaging times
157 and can be considered if time is not a limiting factor.^{22–29}

158 2. Observation of Lymphatic Abnormalities

159 **Absence of contrast uptake:** 5 patients with absent bilateral contrast uptake were also found to have
160 no uptake beyond the ilioinguinal nodes on pedal lymphoscintigraphy. Thus, although considered
161 technical failures, this may in fact be a true finding. It appears possible that those with no uptake on
162 pedal lymphoscintigraphy may be unlikely to show uptake with DCMRL although numbers are too
163 small to make definitive conclusions. Of the 9 patients in whom contrast uptake was absent on one
164 side, this may be due to an absence, functional aplasia or hypoplasia of the lymphatic system,
165 technical failure to access the lymph nodes, or needle displacement. Hypoplastic or absent lymphatics
166 has been shown to be useful for confirming or completing the clinical diagnosis in conditions with
167 primary lymphatic anomalies.³⁰

168 **Dynamic aspect of DCMRL allows for more detailed study of flow in the lymphatics and**
169 **therapy compared to non-contrast MR imaging and lymphoscintigraphy.** For example, 3 of the
170 patients found to have reflux into the contralateral side was not known about prior to DCMRL. Two
171 of these patients subsequently underwent glue embolization [**Figure 5**] with improvement in number
172 of lymphatic blisters and volume of chylous leak, and no further episodes of infection on the affected
173 side in both patients.³¹

174 5 patients demonstrated superficial re-routing of the lymphatics confirming obstruction of their
175 normal lymphatic pathways [**Figure 6** and **Table 2**]. Confirmation of central lymphatic obstruction
176 can then lead to exploration of surgical options such as lymphovenous anastomosis.^{32,33}

177 An inherent difficulty arising from investigating rare diseases is the relatively small numbers of
178 patients with each condition, however the imaging has led to improved understanding of the
179 mechanisms behind lymphatic anomalies and changes in patient management. The development of the
180 technique has resulted in refinements over time which has made the data more heterogenous. Our
181 experience is presented here to facilitate the development of DCMRL services elsewhere within the
182 UK.

183 **Conclusion**

184 DCMRL has proven to be a safe technique for imaging the central lymphatic anatomy of patients with
185 primary lymphatic anomalies without any adverse effects that were observed with lipiodol
186 lymphangiography. Increased uptake of this imaging modality will be invaluable in the phenotyping,
187 classification, and management of patients with primary lymphatic anomalies.

188

189 **References**

- 190 1. Ramirez-Suarez KI, Tierradentro-Garcia LO, Smith CL, *et al.* Dynamic contrast-enhanced
191 magnetic resonance lymphangiography. *Pediatr Radiol* 2022;**52**(2):285–94.
192 <https://doi.org/10.1007/s00247-021-05051-6>.
- 193 2. Bordonaro V, Ciancarella P, Ciliberti P, *et al.* Dynamic contrast-enhanced magnetic resonance
194 lymphangiography in pediatric patients with central lymphatic system disorders. *Radiol Med*
195 2021;**126**(5):737–43. <https://doi.org/10.1007/s11547-020-01309-5>.
- 196 3. Chavhan GB, Lam CZ, Greer MLC, Temple M, Amaral J, Grosse-Wortmann L. Magnetic
197 Resonance Lymphangiography. *Radiol Clin North Am* 2020;**58**(4):693–706.
198 <https://doi.org/10.1016/j.rcl.2020.02.002>.
- 199 4. Browse NL, Burnand KG, Mortimer PS. *Diseases of the lymphatics*. 1. publ. London: Arnold;
200 2003.
- 201 5. Li D, Wenger TL, Seiler C, *et al.* Pathogenic variant in EPHB4 results in central conducting
202 lymphatic anomaly. *Hum Mol Genet* 2018;**27**(18):3233–45.
203 <https://doi.org/10.1093/hmg/ddy218>.
- 204 6. Liu M, Smith CL, Biko DM, *et al.* Genetics etiologies and genotype phenotype correlations in a
205 cohort of individuals with central conducting lymphatic anomaly. *Eur J Hum Genet*
206 2022;**30**(9):1022–8. <https://doi.org/10.1038/s41431-022-01123-9>.
- 207 7. Byrne AB, Brouillard P, Sutton DL, *et al.* Pathogenic variants in *MDFIC* cause recessive central
208 conducting lymphatic anomaly with lymphedema. *Sci Transl Med* 2022;**14**(634).
209 <https://doi.org/10.1126/scitranslmed.abm4869>.
- 210 8. Biko DM, Reisen B, Otero HJ, *et al.* Imaging of central lymphatic abnormalities in Noonan
211 syndrome. *Pediatr Radiol* 2019;**49**(5):586–92. <https://doi.org/10.1007/s00247-018-04337-6>.
- 212 9. Gordon K, Varney R, Keeley V, *et al.* Update and audit of the St George’s classification
213 algorithm of primary lymphatic anomalies: A clinical and molecular approach to diagnosis. *J*
214 *Med Genet* 2020;**57**(10):653–9. <https://doi.org/10.1136/jmedgenet-2019-106084>.
- 215 10. Patel S, Hur S, Khaddash T, Simpson S, Itkin M. Intranodal CT Lymphangiography with Water-
216 soluble Iodinated Contrast Medium for Imaging of the Central Lymphatic System. *Radiology*
217 2022;**302**(1):228–33. <https://doi.org/10.1148/radiol.2021210294>.
- 218 11. Rabinowitz D, Dysart K, Itkin M. Neonatal lymphatic flow disorders: central lymphatic flow
219 disorder and isolated chylothorax, diagnosis and treatment using novel lymphatic imaging
220 and interventions technique. *Curr Opin Pediatr* 2022;**34**(2):191–6.
221 <https://doi.org/10.1097/MOP.0000000000001109>.
- 222 12. Pieper CC, Wagenpfeil J, Henkel A, *et al.* MR lymphangiography of lymphatic abnormalities in
223 children and adults with Noonan syndrome. *Sci Rep* 2022;**12**(1).
224 <https://doi.org/10.1038/s41598-022-13806-w>.

- 225 13. Nadolski GJ, Itkin M. Feasibility of Ultrasound-guided Intranodal Lymphangiogram for
226 Thoracic Duct Embolization. *Journal of Vascular and Interventional Radiology*
227 2012;**23**(5):613–6. <https://doi.org/10.1016/j.jvir.2012.01.078>.
- 228 14. Nadolski GJ, Ponce-Dorrego MD, Darge K, Biko DM, Itkin M. Validation of the Position of
229 Injection Needles with Contrast-Enhanced Ultrasound for Dynamic Contrast-Enhanced MR
230 Lymphangiography. *Journal of Vascular and Interventional Radiology* 2018;**29**(7):1028–30.
231 <https://doi.org/10.1016/j.jvir.2018.02.034>.
- 232 15. Hur S, Kim J, Ratnam L, Itkin M. Lymphatic Intervention, the Frontline of Modern Lymphatic
233 Medicine: Part I. History, Anatomy, Physiology, and Diagnostic Imaging of the Lymphatic
234 System. *Korean J Radiol* 2023;**24**(2):95–108. <https://doi.org/10.3348/kjr.2022.0688>.
- 235 16. Rane S, Donahue PMC, Towse T, *et al.* Clinical Feasibility of Noninvasive Visualization of
236 Lymphatic Flow with Principles of Spin Labeling MR Imaging: Implications for Lymphedema
237 Assessment. *Radiology* 2013;**269**(3):893–902. <https://doi.org/10.1148/radiol.13120145>.
- 238 17. Bernstein MA, King KF, Zhou XJ. COMMON IMAGE RECONSTRUCTION TECHNIQUES.
239 *Handbook of MRI Pulse Sequences*. Elsevier; 2004;491–571. [https://doi.org/10.1016/B978-](https://doi.org/10.1016/B978-012092861-3/50019-4)
240 [012092861-3/50019-4](https://doi.org/10.1016/B978-012092861-3/50019-4).
- 241 18. Gooty VD, Veeram Reddy SR, Greer JS, *et al.* Lymphatic pathway evaluation in congenital
242 heart disease using 3D whole-heart balanced steady state free precession and T2-weighted
243 cardiovascular magnetic resonance. *J Cardiovasc Magn Reson* 2021;**23**(1):16.
244 <https://doi.org/10.1186/s12968-021-00707-6>.
- 245 19. The Royal College of Radiologists. Guidance on gadolinium-based contrast
246 agent administration to adult patients. The Royal College of Radiologists 2019. Retrieved
247 from [https://www.rcr.ac.uk/our-services/all-our-publications/clinical-radiology-](https://www.rcr.ac.uk/our-services/all-our-publications/clinical-radiology-publications/guidance-on-gadolinium-based-contrast-agent-administration-to-adult-patients)
248 [publications/guidance-on-gadolinium-based-contrast-agent-administration-to-adult-patients](https://www.rcr.ac.uk/our-services/all-our-publications/clinical-radiology-publications/guidance-on-gadolinium-based-contrast-agent-administration-to-adult-patients)
- 249 20. Rohrer M, Bauer H, Mintorovitch J, Requardt M, Weinmann H-J. Comparison of magnetic
250 properties of MRI contrast media solutions at different magnetic field strengths. *Invest Radiol*
251 2005;**40**(11):715–24. <https://doi.org/10.1097/01.rli.0000184756.66360.d3>.
- 252 21. Biko DM, Smith CL, Otero HJ, *et al.* Intrahepatic dynamic contrast MR lymphangiography:
253 initial experience with a new technique for the assessment of liver lymphatics. *Eur Radiol*
254 2019;**29**(10):5190–6. <https://doi.org/10.1007/s00330-019-06112-z>.
- 255 22. Mills M, van Zanten M, Borri M, *et al.* Systematic Review of Magnetic Resonance
256 Lymphangiography From a Technical Perspective. *Journal of Magnetic Resonance Imaging*
257 2021;**53**(6):1766–90. <https://doi.org/10.1002/jmri.27542>.
- 258 23. Mazzei MA, Gentili F, Mazzei FG, *et al.* High-resolution MR lymphangiography for planning
259 lymphaticovenous anastomosis treatment: a single-centre experience. *Radiol Med*
260 2017;**122**(12):918–27. <https://doi.org/10.1007/s11547-017-0795-x>.

- 261 24. Krishnamurthy R, Hernandez A, Kavuk S, Annam A, Pimpalwar S. Imaging the central
262 conducting lymphatics: Initial experience with dynamic MR lymphangiography. *Radiology*
263 2015;**274**(3):871–8. <https://doi.org/10.1148/radiol.14131399>.
- 264 25. Itkin MG, McCormack FX, Dori Y. Diagnosis and treatment of lymphatic plastic bronchitis in
265 adults using advanced lymphatic imaging and percutaneous embolization. *Ann Am Thorac Soc*
266 2016;**13**(10):1689–96. <https://doi.org/10.1513/AnnalsATS.201604-292OC>.
- 267 26. Dori Y, Keller MS, Fogel MA, *et al.* MRI of lymphatic abnormalities after functional single-
268 ventricle palliation surgery. *American Journal of Roentgenology* 2014;**203**(2):426–31.
269 <https://doi.org/10.2214/AJR.13.11797>.
- 270 27. Mohanakumar S, Telinius N, Kelly B, *et al.* Morphology and Function of the Lymphatic
271 Vasculature in Patients With a Fontan Circulation. *Circ Cardiovasc Imaging*
272 2019;**12**(4):e008074. <https://doi.org/10.1161/CIRCIMAGING.118.008074>.
- 273 28. Dori Y, Keller MS, Rome JJ, *et al.* Percutaneous lymphatic embolization of abnormal
274 pulmonary lymphatic flow as treatment of plastic bronchitis in patients with congenital heart
275 disease. *Circulation* 2016;**133**(12):1160–70.
276 <https://doi.org/10.1161/CIRCULATIONAHA.115.019710>.
- 277 29. Suga K, Yuan Y, Ogasawara N, Okada M, Matsunaga N. Localization of breast sentinel lymph
278 nodes by MR lymphography with a conventional gadolinium contrast agent. Preliminary
279 observations in dogs and humans. *Acta Radiol* 2003;**44**(1):35–42.
- 280 30. Uchida T, Uchida Y, Takahashi M, *et al.* Yellow nail syndrome in which intranodal
281 lymphangiography contributed to the diagnosis. *Internal Medicine* 2021;**60**(22):3599–603.
282 <https://doi.org/10.2169/internalmedicine.6499-20>.
- 283 31. Pieper CC, Hur S, Sommer C-M, *et al.* Back to the Future. *Invest Radiol* 2019;**54**(9):600–15.
284 <https://doi.org/10.1097/RLI.0000000000000578>.
- 285 32. Othman S, Azoury SC, Klifto K, Toyoda Y, Itkin M, Kovach SJ. Microsurgical Thoracic Duct
286 Lymphovenous Bypass in the Adult Population. *Plast Reconstr Surg Glob Open*
287 2021;**9**(10):e3875. <https://doi.org/10.1097/gox.0000000000003875>.
- 288 33. Weissler JM, Cho EH, Koltz PF, *et al.* Lymphovenous anastomosis for the treatment of
289 chylothorax in infants: A novel microsurgical approach to a devastating problem. *Plast*
290 *Reconstr Surg* 2018;**141**(6):1502–7. <https://doi.org/10.1097/PRS.0000000000004424>.

291

292

293 **Figures**

294 **Figure 1.** Comparison of non contrast and DCMRL images of the iliac and lumbar lymphatics in a 30-year-old
295 female patient (Case 19) with unilateral right leg lymphoedema. Images shown are over the abdomen and pelvis
296 from the lower lumbar vertebrae to the level of the femoral heads. The lymphatics (white arrows) are faintly
297 visualised on the T₂-weighted non-contrast imaging, with a central slice of the 3D acquisition shown here (1a)
298 and seen much more clearly on the post contrast T₁-weighted imaging, as demonstrated in this MIP SPOILED
299 GRADIENT ECHO image (1b). DCMRL showed normal central lymphatics with good bilateral drainage.

300

301

Journal Pre-proof

302

303 **Figure 2. One of two patients in whom lymphatics were visualised on non-contrast imaging is a** 64-year-
304 old male patient (Case 28) with chylous reflux into right thigh and genitalia, and right thigh and genital
305 lymphoedema. The first image encompasses the lower thorax to the level of the femoral heads. Markedly dilated
306 lymphatics (white arrow) are reasonably well seen on the non-contrast T₂ images, as can be seen in the single
307 central slice of the 3D acquisition shown **(2a)** **The same dilated lymphatic channel is shown in the post**
308 **contrast image (black arrow)** . Contrast was only injected from left groin as nodes had been surgically
309 removed on the right. However, significant reflux into the right side was identified (white arrow) on post
310 contrast T₁-weighted SPRG image, displayed in MIP form here **(2b)**. Dynamic imaging demonstrated the
311 opacification of the right sided channels after injection of contrast from the left.

312

313

Journal Pre-proof

314 **Figure 3.** T₂ weighted images of a patient (25-year-old female, Case 8), with enlarged inguinal lymphatic
315 vessels. (3a) shows the MIP resulting from the 2D T₂-weighted TSE sequences, while (3b) is a mid-image slice
316 from this sequence. (3c) and (3d) are the equivalent from the 3D heavily T₂-weighted sequence. Note that while
317 more of the anatomy is visible in a-b, the reduced background signal improves lymphatic vessels and fluid
318 pooling visibility with the 3D acquisition (c-d). Note too that visualisation of lymphatic vessels is rarer in the
319 more moderately 2D T₂-weighted images (a-b) than the 3D (c-d). The arrows highlight lymphatics in the upper
320 thigh on the patient's left.

321

322

323

324

325

326

327

328

329

330

331

332

333

334

335

336

337

338 **Figure 4.** Post contrast T₁ weighted Dixon maximum-intensity projection (MIP) of a 24-year-old male patient
339 (Case 14) with no drainage into normal lymphatic vessels showing superficial rerouting of contrast injected into
340 a right groin lymph node (thick white arrow shows contrast partially extravasated around the right groin lymph
341 node) up the right flank (thin white arrow showing contrast re-routing along right flank).

342

343

344

345

346

347

348

Journal Pre-proof

349 **Figure 5.** Glue embolization carried out on a patient with reflux (Case 28 from **Figure 2**). Lipiodol
350 lymphangiogram first carried out with injection from left groin lymph node. Refluxing channels targeted
351 fluoroscopically and glue embolization (thin white arrow shows glue cast in embolized lymphatics) carried out
352 after microcatheter (white arrow) catheterisation of the lymphatic vessels.

353

354

Journal Pre-proof

355

356 **Figure 6.** 66-year-old male patient (Case 28) with right leg and genital lymphoedema. Previous surgery with
357 removal of right groin lymph nodes thus only the left was injected. Post contrast maximum-intensity projection
358 (MIP) shows contrast injected from left groin node (black arrow) has refluxed to the right, then rerouting around
359 the right flank (white arrow shows refluxed contrast starting to track up right flank) **(6a)**. Delayed imaging
360 showed the contrast from the right flank tracking up the chest wall (white arrow) before draining via further
361 collaterals into the TD (black arrow) **(6b)**. Images shown were acquired with the Dixon technique.

362

363

364

Journal Pre-proof

Table 1. Typical imaging parameters for magnetic resonance lymphangiography at 3.0 T. Note that field of view and acquisition matrix varied from participant to participant based on the anatomy. Image acquisition times varied based on the field of view required for adequate anatomical coverage but were generally between 6 – 10 minutes for the heavily T₂-weighted and 0.5-1 minutes per volume for the dynamic T₁-weighted series.

TR: repetition time, TE: echo time, FA: flip angle, NSA: number of signal averages, SENSE factor: SENSitivity Encoding

	TR / TE (ms)	FA (°)	Reconstructed Voxel Size (mm)	NSA	Fat Suppression	Motion Reduction	SENSE Factor (Direction)	Typical acquisition time	Features of interest
Pre-contrast:									
Coronal 2D T ₂ -weighted TSE	'shortest' * / 80 ms	90	0.78 x 0.78 x 4.00	1	SPAIR	Breath-held	2.0 (RL)	5 min	Fluid accumulations (e.g., ascites), anatomy, incidental findings
Coronal 3D heavily T ₂ -weighted TSE	3200 / 740	90	0.90 x 0.90 x 1.50	2	SPAIR	N/A	1.6 (RL) 1.6 (AP)	9 min	Fluid accumulations, occasionally LV
Coronal 3D T ₁ -weighted SPOILED GRADIENT ECHO	'shortest' / 'shortest' *	30	0.76 x 0.76 x 1.50	1	N/A	N/A	3.0 (RL)	0.5 min	Baseline prior to contrast injection
Post-contrast:									
Coronal 3D T ₁ -weighted SPOILED GRADIENT ECHO	'shortest' / 'shortest' *	30	0.76 x 0.76 x 1.50	1	N/A	N/A	3.0 (RL)	0.5 min / dynamic	Enhancing LV, and contrast leakage/pooling
Coronal 3D T ₁ -weighted Dixon	4.36 / 1.41 / 2.60 †	10	0.71 x 0.71 x 1.00	1	Dixon	N/A	1.6 (RL) 1.6 (AP)	2 min	Enhancing LV, and contrast leakage/pooling

* 'shortest' TR for the Coronal 2D T₂-weighted TSE was approx. 2000ms; 'shortest' TR / TE for the Coronal 3D T₁-weighted spoiled gradient echo were approx. 5 / 2 ms.

† TE₁ = 1.41ms, TE₂ = 2.60ms.

RL: Right – Left; AP: Anterior – Posterior; LV: lymphatic vessels

Table 2. Summary of patients and DCMRL findings

Patient No	Sex	Age at time of study (years)	Lymphatic Diagnosis	Unilateral Injection	Bilateral injection with no uptake	Bilateral injection with bilateral uptake	Bilateral injection with unilateral uptake
1	M	18	WILD syndrome [22]		x		
2	M	38	WILD syndrome		x		
3	M	31	RASopathy (Noonan syndrome)			TD terminates at ligation.	
4	F	39	RASopathy (Noonan syndrome)				Mediastinal, pleural & pericardial leak.
5	F	50	YNS			Normal central lymphatics.	
6	M	61	YNS			Absent TD, collateral filling, LPSA.	
7	F	47	GLD			Dilated lymphatic vessels.	
8	F	25	GLD			Absent TD, collateral filling.	
9	M	46	GLD		x		
10	M	19	GLD	CL severe oedema. CL contrast- reflux.			

11	F	70	GLD			Obstruction with rerouting and filling of distal TD.	
12	M	31	GLD				LPSA, absent lower TD (ligated). Distal filling via collaterals.
13	M	42	GLD	CL severe oedema. Superficial rerouting.			
14	M	24	<i>ERG</i> -related GLD [23]				Obstruction with rerouting to TD.
15	F	41	<i>ERG</i> -related GLD		x		
16	M	29	SCIDS			Normal central lymphatics.	
17	M	38	Unilateral leg lymphoedema (R)		x		
18	F	16	Unilateral leg lymphoedema (L)				Absent TD, collateral filling.
19	F	30	Unilateral leg lymphoedema (R)			Normal central lymphatics.	
20	F	39	Unilateral leg lymphoedema (L)	CL severe oedema. Normal on side of uptake and centrally.			
21	F	25	Unilateral leg lymphoedema (L)				Normal on side of uptake and centrally.
22	M	29	Left perineal lymphovascular malformation				Normal on side of uptake and centrally.
23	M	33	Left hindquarter lymphovascular malformation, chylous reflux, lymph leakage				Ipsilateral reflux to pelvis and leg.
24	F	52	Bilateral lower limb and abdominal wall lymphoedema, chylous				LPSA, dilated TD with distal TD obstruction.

			ascites & pleural effusions.				
25	M	34	Unilateral leg lymphoedema (L), chylous ascites & pleural effusions			Absent distal TD, LPSA.	
26	M	62	Genital and right leg lymphoedema, chylous reflux, lymph leakage	CL surgery. CL contrast- reflux.			
27	M	17	Genital and bilateral lower limb lymphoedema				Obstruction with rerouting to CC.
28	M	64	Genital and right leg lymphoedema, chylous reflux, lymph leakage	CL surgery. CL contrast- reflux.			

Abbreviation Key

CC - Cisterna chyli

CL - Contralateral

GLD - Generalised Lymphatic Dysplasia

L – left

LPSA - Lymphopseudoaneurysm

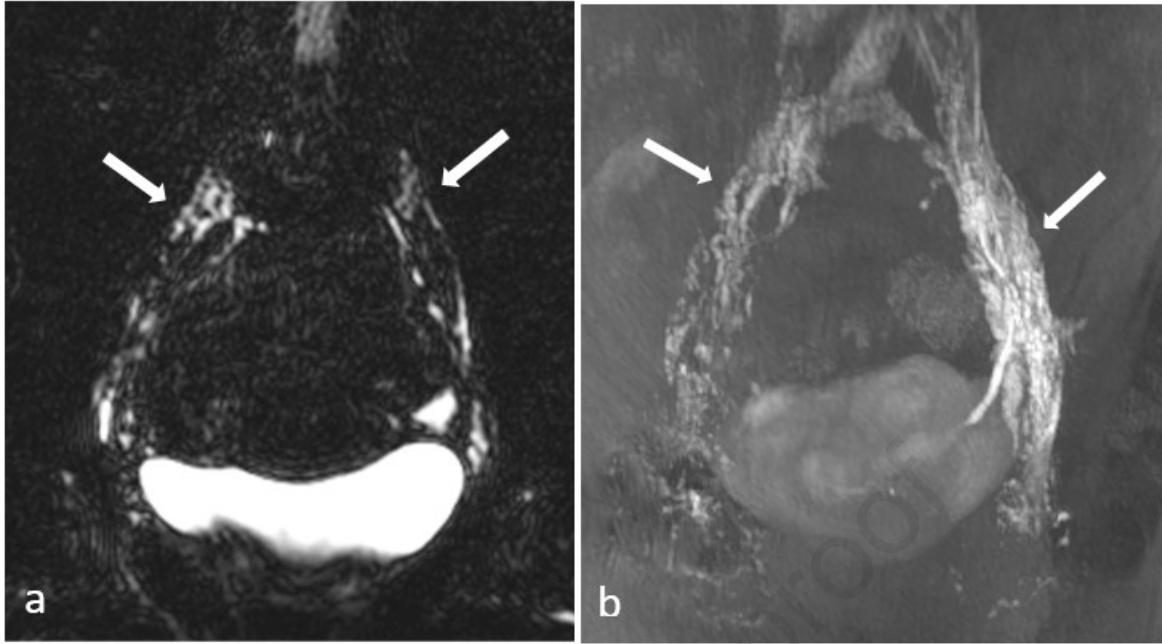
R - right

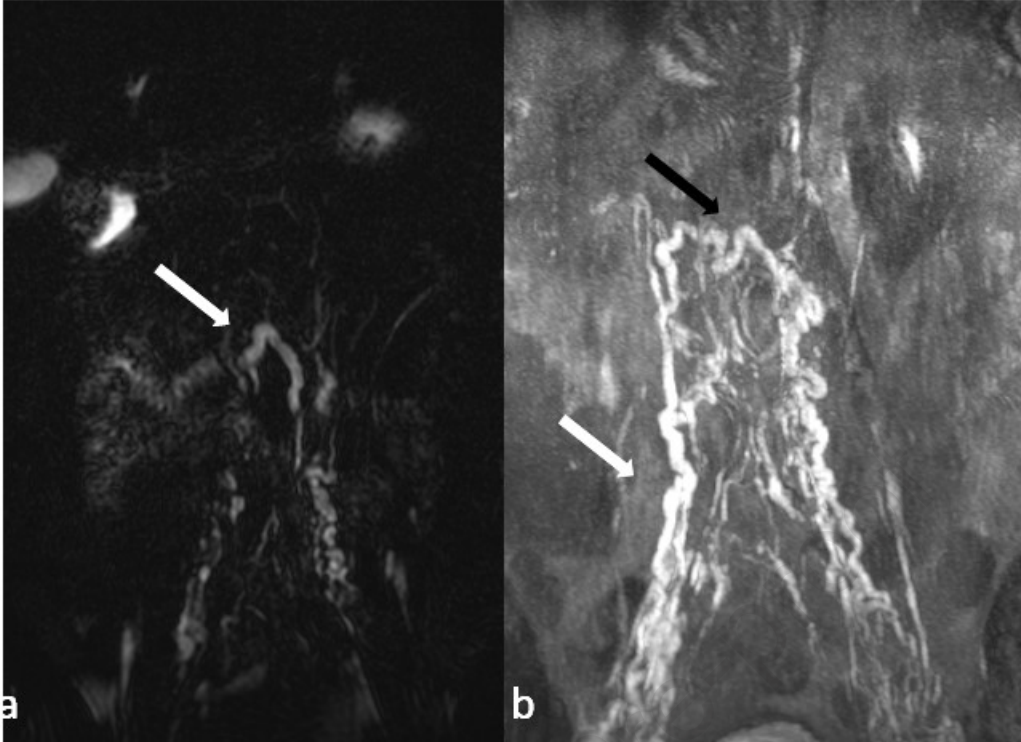
SCIDS - Severe combined immunodeficiency syndrome

TD - Thoracic duct

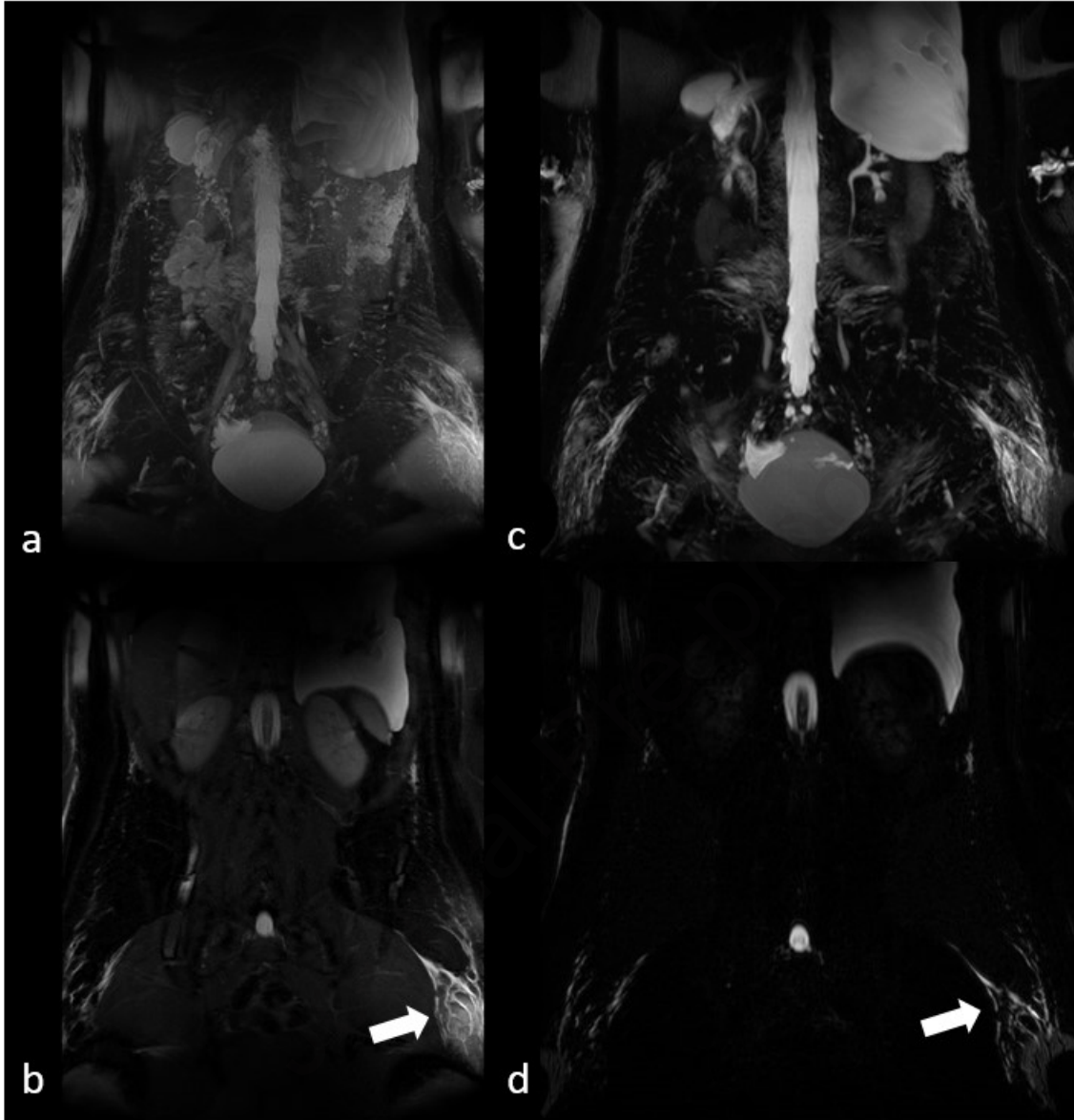
WILD – Warts, Immunodeficiency, Lymphoedema and anogenital Dysplasia

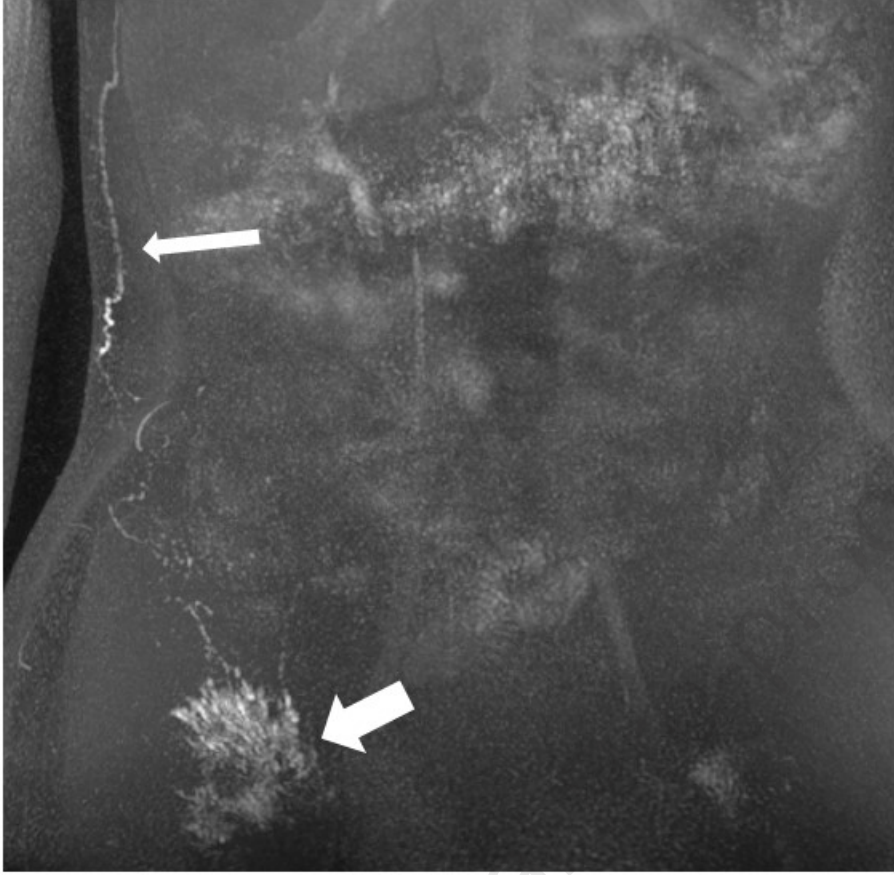
YNS - Yellow Nail Syndrome



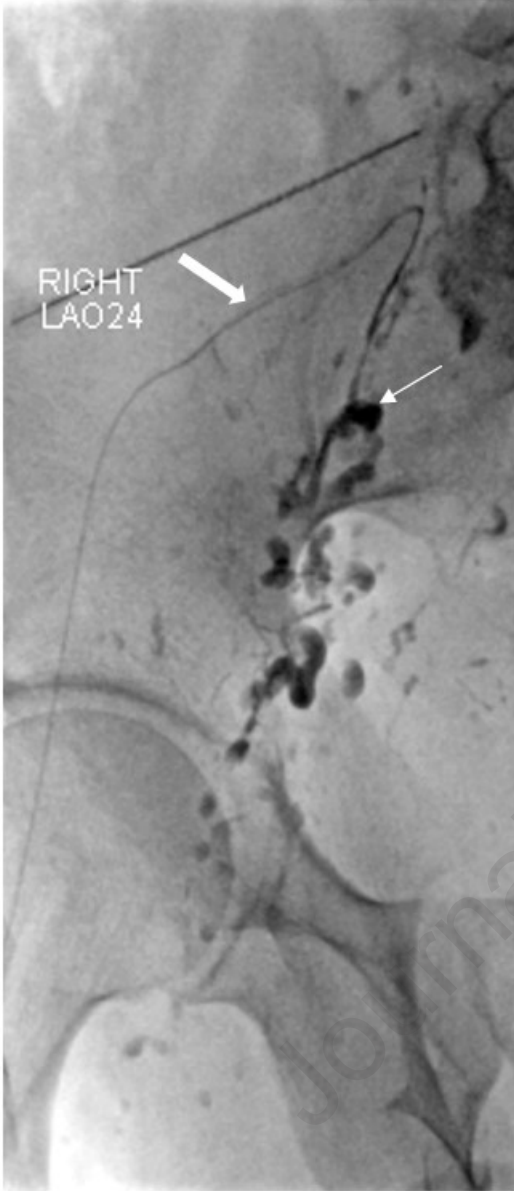


Journal Pre-proof





Journal





Journal Pre-proof

Highlights:

1. Central lymphatics visualised in 82.1% with DCMRL
2. Optimising imaging parameters and needle placement technique are critical
3. DCMRL enables dynamic assessment of central lymphatics with anatomical correlation

Journal Pre-proof

Declaration of interests

The authors declare that they have no known competing financial interests or personal relationships that could have appeared to influence the work reported in this paper.

The authors declare the following financial interests/personal relationships which may be considered as potential competing interests:

L A Ratnam reports financial support was provided by UKRI Medical Research Council. If there are other authors, they declare that they have no known competing financial interests or personal relationships that could have appeared to influence the work reported in this paper.